IEEE Access
Multidisciplinary | Rapid Review | Open Access Journal

Received December 9, 2020, accepted December 22, 2020, date of publication January 6, 2021, date of current version January 26, 2021.

Digital Object Identifier 10.1109/ACCESS.2020.3049081

A Fuzzy Logic Based Piezoresistive/Piezoelectric Fusion Algorithm for Carbon Nanocomposite Wide Band Strain Sensor

AHMED ALOTAIBI[1] AND SOHEL ANWAR[2]
[1]School of Mechanical Engineering, Purdue University, West Lafayette, IN 47906, USA
[2]Department of Mechanical and Energy Engineering, Indiana University–Purdue University Indianapolis, Indianapolis, IN 46202, USA

Corresponding author: Sohel Anwar (soanwar@iupui.edu)

The work of Sohel Anwar was supported by the research funds of IUPUI.

ABSTRACT Polymer nanocomposites (PNC) have a great potential for in-situ strain sensing applications in both static and dynamic loading scenarios. These PNCs, having a polymer matrix of polyvinylidene fluoride (PVDF) with a conductive filler of multi-walled carbon nanotubes (MWCNT), have both piezoelectric and piezoresistive characteristics. Generally, this composite would accurately measure either low frequency dynamic strain using piezoresistive characteristic or high frequency dynamic strains using piezoelectric characteristics of the MWCNT/PVDF film sensor. This limits the frequency bands of the strain sensor to either piezoresistive or piezoelectric ranges. In this study, a novel weighted fusion technique, called piezoresistive/piezoelectric fusion (PPF), is proposed to combine both piezoresistive and piezoelectric characteristics to capture wide frequency bands of strain measurements in real time. This fuzzy logic (FL) based method combines the salient features (i.e. piezoresistive and piezoelectric) of the nanocomposite sensor via reasonably accurate models to extend the frequency range over a wider band. The FL determines the weight of each signal based on the error between the estimate and actual measurements. These weights indicate the contribution of each signal to the final fused measurement. The fuzzy inference system (FIS) was developed using both optimization and data clustering techniques. In addition, type-2 FIS was utilized to overcome the model's uncertainty limitations. The developed PPF methods were verified with experimental data at different dynamic frequencies that were obtained from existing literature. The fused measurements of the MWCNT/PVDF were found to correlate very well with the actual strain and a high degree of accuracy was achieved by the subtractive clustering PPF's FISs algorithm.

INDEX TERMS PPF, frequency band, fusion, fuzzy logic, nanocomposite, piezoelectric, piezoresistive, strain sensor, wide band.

I. INTRODUCTION

Sensors are fundamental and essential in many applications such as biochemical and medical diagnosis [1], [2], industrial and fabrication processes [3], and environmental and structure health monitoring [4], [5]. A sensor converts a physical phenomenon into an electrical signal, which is processed and calibrated for accurate and reliable measurements. The 21st century industrial revolution demands that new sensors be developed to advance technologies in manufacturing with higher accuracy, quality, and capacity. Strain and force sensors have gained much attention in recent years due to their broad applications for surgical robot [6], polishing machine [7], biomedical and physical therapy instruments [8]–[11].

Recently, Polymer nanocomposites (PNCs) have attracted much attention in the materials science and engineering fields. In this type of composites, a polymer matrix is combined with non-organic fillers, one of which is in a nanoscale dimension. The resultant composite retains both the polymer and filler advantages. Carbon nanotubes (CNTs) were discovered in 1991 by Iijima [12], greatly advancing the nanocomposite materials field. CNTs properties have been extensively investigated by many researchers. They have been shown to possess extraordinary mechanical [13], [14], electrical [15], [16], optical [15], and thermal [14], [17], [18] properties. In addition, they have one dimensional structure and high aspect ratio (length-to-diameter ratio), making them

The associate editor coordinating the review of this manuscript and approving it for publication was Wai-Keung Fung.

unique fillers to produce electrically conductive PNCs [19]. As a result, high conductivity PNCs can be achieved with lower concentration of CNT compared with other conductive nano-fillers. The percolation threshold defines the percentage concentration of the conductive nano-filler inside the composite at which the electrical resistivity of the composite increases significantly [20]. In addition, the percolation threshold is greatly influenced by the aspect ratio of the nano filler inside the composites [21], [22]. The volume fraction, conductivity and topology of the nano filler networks, and interaction between the polymer and fillers control the PNC's overall conductivity [23], [24]. For strain measurement, the PNC-CNT's piezoresistivity is influenced by the demolition of the conductive networks, tunneling resistance, and the changes of the CNT piezoresistivity [25]. However, the latter is less influenced due to the relatively small change in resistance [26]. The tunneling resistance occurs between the crossings or the neighboring of the CNTs, and it is the most dominant factor in the overall composite conductivity [27].

In terms of polymer matrix, polyvinylidene fluoride (PVDF) has been widely studied and used for piezoelectricity based sensing and actuation applications due to their affordable cost, mechanical characteristics, and chemical stability. PVDF has been utilized in force/pressure sensing, energy harvesting, humidity and gas flow sensors, and acoustic and ultrasonic sensors [28]–[34]. Several researchers have investigated the advantages of mixing CNT with PVDF. The presence of multi walled CNTs (MWCNTs) advances the electromechanical characteristics of the composite [35]. In addition, the activation of the piezoelectric properties of the MWCNT/PVDF films were achieved at lower voltages due to the presence of the CNT, whereas the PVDF films needs higher voltages [36]. Moreover, CNTs change conformations of the semi-crystalline structure from α phase to β phase, where the highest polarization can be achieved [37].

The MWCNT/PVDF composite film is a unique sensing element, which can measure strain using either piezoresistive or piezoelectric properties. The piezoresistive strain measurement is appropriate for static or low loading frequencies. In contrast, piezoelectric strain measurement can capture high frequency measurements with higher sensitivity and accuracy. The piezoresistivity of the composite film was characterized by Zeng *et al.* [38] who reported that a hot pressed 1 wt.% MWCNT/PVDF film was less sensitive at high frequency (2000 Hz) compared to 6.5 wt.% carbon black (CB)/PVDF strain sensor. Another study has shown that 1 wt.% MWCNT/PVDF film failed to match the output from 1 wt.% Graphene/PVDF and 6 wt.% CB/PVDF films at 200 Hz dynamic loading [39]. For piezoelectric measurement, a sandwiched MWCNT/PVDF film between two polypropylene (PP) films was tested under compression loading ranging from 200 N to 350 N at low frequency (0.5 Hz) [40]. The piezoelectric output voltage was relatively small at a high magnitude force of 200 N. A mechanically stretched and electrically poled (corona poling) PVDF/MWCN strain sensor that is frequency dependent was reported by Sanati *et al.* [41]. For strain measurement bellow 5 Hz, the piezoresistive sensing provided good accuracy whereas piezoelectric sensing offered good accuracy for strain measurements above 5 Hz up to 1000 Hz [41]. For optimal piezoresistive and piezoelectric strain sensing performance, 0.1 wt.% and 2 wt.% of CNT exhibited better accuracy, respectively [41].

The frequency dependent strain measurements are affected by multi-label parameters such as the composite's electrical, mechanical, and physical properties. In terms of piezoresistivity, the gauge factor (GF) and the matrix's mechanical response places an upper bound on the measurement's amplitude at high frequencies [38]. In addition, the complex viscosity of a compressed molded MWCNT/PVDF composite sample decreases with increasing frequency [42]. That would limit the movement of the CNTs with respect to each other and reduce the tunneling resistance changes. Nevertheless, the carbon nanofiller volume fraction and dispersion, which are affected by the fabrication process, have a significant effect on the sensors' performances. For piezoelectricity, the strain coefficient D33 is greater than D31 for lead zirconate titanate (PZT) and PVDF materials. As a result, the resonant frequency mode of D33 limits the measurements at which low frequency vibration is desirable [43].

Researchers attempted to combine both piezoresistive and piezoelectric characteristics to capture both static and dynamic mechanical stimulation using stake fabrication process. He *et al.* [44] introduced a multi-layered piezoelectric-piezoresistive tactile sensor. The sensor consisted of three electrodes layers: a piezoelectric layer, a piezoresistive layer, and a common electrode layer. The piezoelectric and piezoresistive layers were made of PVDF (-TrFE) and MWCNTs/ Polyurethane (PU). Similarly, Khan *et al.* [45] reported two multi-layered pressure sensors made from (PVDF-TrFE) and (PVDF-TrFE)-MWCNTs sensing materials using screen printing technology. These studies introduced sensors that have the capability to measure static and dynamic measurements. However, each measurement was performed with fixed connections or setup: either static or dynamic.

Sanati *et al.* [41] proposed a fusion methodology for the piezoelectric and piezoresistive MWCNT/PVDF nanocomposite sensors. The technique is analogous to an optimum linear smoother developed by Fraser and Potter in 1969, which combines two optimal linear filters or estimates [46]. The fusion equation uses piezoelectric and piezoresistive signals, compensation coefficients, and their covariances to compute the final fused signal [41]. The compensation coefficients were fixed during the transitioning frequencies (5 - 160 Hz) bands, which might lead to losing measurement data and exclude any resonant frequency effects. An accurate and robust frequency based fusion method for real-time strain measurement is needed to overcome the stated limitation and disadvantages of previous attempts to combine both piezoresistive and piezoelectric characteristics.

Sensor fusion is a methodology that combines multiple sensory measurements, which could be of similar or different types of signals and are not sufficient by themselves to provide a useful output. Data fusion may be necessary in different applications such as, military applications, law enforcement, remote sensing, automated monitoring of equipment, medical diagnosis, and robotics [47]. Any sensor measurements are subject to limitations such as the measurement being restricted in a narrower area of the broad environment [48]. Similarly, image fusion is the process of combining different images' features and produce a higher quality image [49]. Fuzzy set theory has been implemented in different image processing and image fusion algorithms. A novel image fusion algorithm, which based on two-scale image decomposition integrated with fuzzy set theory and image morphology, was introduced by Jiang *et al.* [49]. They presented a new fusion method based on non-subsampled contourlet transform (NSCT) with intuitionistic fuzzy sets for the infrared and visible image fusion [50]. Yang *et al.* proposed a novel multimodal sensor medical image fusion method based on type-2 fuzzy logic in NSCT domain [51]. The image fusion method has retained more informative and higher quality fused medical images by utilizing the fuzzy logic. The fuzzy set based image fusion's algorithms have shown more effective fusion performance than other conventional image fusion methods [52].

In the current strain sensing technology, the piezoresistive and piezoelectric characteristics are sensitive and accurate at low and high frequency measurements, respectively. A Kalman Filter Fuzzification (KFF) is used for measurement estimation of position, velocity, and acceleration of 3D target tracking application [53]. In this method, the Kalman filter (KF) estimated the state for each measurement and associated each estimate with different scaler weights [54], [55]. These weights define the contribution of each signal to the final fused state. They are generated by the fuzzy inference system (FIS) for both sensors based on the calculated normalized errors between the estimates and the actual measurements. Sensor fusion is a great tool to advance and improve the MWCNT/PVDF strain sensors' sensitivity by combining both characteristics using more sophisticated fusion method.

Despite the fact that MWCNT/PVDF strain sensors' characteristics are frequency dependent, few researchers have addressed these limitation and sensor fusion of these characteristics not been dealt with in depth. The aims of this work are to overcome the piezoresistive and piezoelectric characteristic frequency dependent limitation using a weighted combination of both measurements when it is necessary. Here a novel fuzzy logic based PPF fusion method has been designed, developed, and verified with experimental data at different dynamic frequencies that were presented in the Park *et al.* study [41]. This technique can be generalized to any other sensor fusion methods where their performances are frequency dependent. Finally, the uniqueness of this work is that it is a frequency-based real-time measurements fusion method that efficiently weights each signal to achieve an accurate estimate. Most prior research on such sensors studied their performance under fixed measurement setup, e.g. either static to low frequency ranges or high frequency ranges. The proposed fusion algorithm has the potential to improve the overall accuracy in fusing both piezoresistive and piezoelectric strain measurements over a wide frequency range for a PNC strain sensor.

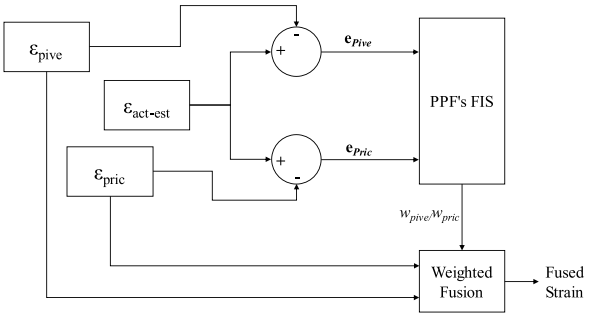

FIGURE 1. Schematic of the Piezoresistive/ Piezoelectric Fusion (PPF) Method.

This article presents a new fusion approach to combine the MWCNT/PVDF sensor's piezoresistive and piezoelectric characteristics and offers a wide band strain sensing methodology. Different strategies were utilized and implemented to produce the PPFs' FISs such as, optimization method, data clustering, and fuzzy type-2 system. The proposed PPF method were investigated and analyzed for their accuracy and Root Mean Squared Error (RMSE) at different operating frequencies. The subtractive cluster and type-2 FIS based PPF fused both measurements while attaining high accuracy and relatively small RMSEs compared to other strategies. The presented results emphasize the validity of the proposed fusion method.

II. PIEZORESISTIVE/WWWWW/PIEZOELECTRIC FUSION (PPF) METHODS

For the proposed MWCNT/PVDF strain sensor, the PPF method has been developed and implemented to combine the measurement data through a fuzzy logic algorithm and generate a wide band strain output, as shown in Fig. 1. In this method, the piezoresistive and piezoelectric strain data of two adjacent MWCNT/PVDF sensors are used to estimate the final fused strain. While the actual estimated strains ($\varepsilon_{act-est}$) are to be given via Kalman Filter (KF) or the equivalent circuit based models, actual strains were used here to demonstrate the effectiveness of the proposed method. The piezoresistive and piezoelectric measurement errors (e_{Pive} and e_{Pric}) are calculated by subtracting the estimated strain and piezoresistive and piezoelectric strain data, respectively.

The error measurements were normalized using the Min-Max scaling. The normalized error signals are utilized by the fuzzy inference system (FIS) to define the contribution of each signal to the fused strain output as follows:

$$\varepsilon_f\,(k) = w_{Pive}\,(k)\,\varepsilon_{Pive}\,(k) + w_{Pric}\,(k)\,\varepsilon_{Pric}\,(k) \qquad (1)$$

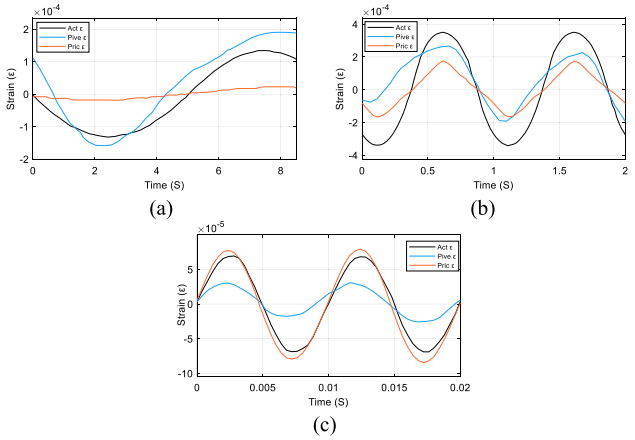

FIGURE 2. Strain measurements at a cantilever using piezoresistive sensor, piezoelectric sensor, and metal foil strain gauge (actual) under forced vibration of: (a) 0.1 Hz, (b) 1 Hz, and (c) 100 Hz [41].

where w_{Pive} and w_{Pric} are the associated weight with the piezoresistive signal (ε_{Pive}) and piezoelectric signal (ε_{Pric}); respectively, in the final fused signal (ε_f). The final fused strain will attempt to match the actual strain (ε_{act}) using the developed FISs. Equation (1) has two unknown weights which would lead to infinite number of solutions for the weights. The dependent weight solutions are shown in equations (2) and (3):

$$w_{Pive} = \frac{\varepsilon_{act} - w_{Pric} \times \varepsilon_{Pric}}{\varepsilon_{Pive}} = \frac{\varepsilon_{act} - w_{Pric}\,(\varepsilon_{act} - e_{Pric})}{\varepsilon_{act} - e_{Pive}} \tag{2}$$

$$w_{Pric} = \frac{\varepsilon_{act} - w_{Pive} \times \varepsilon_{Pive}}{\varepsilon_{Pric}} = \frac{\varepsilon_{act} - w_{Pive}\,(\varepsilon_{act} - e_{Pive})}{\varepsilon_{act} - e_{Pric}} \tag{3}$$

To simplify the fusion equation's solution, one sensor was assigned a constant weight while the other sensor's weight was computed using either (2) or (3) based on both sensors' accuracy at that frequency. At low frequency strain measurements, w_{Pive} was assigned a full weight of one and w_{Pric} was computed using (3) due to the high accuracy and sensitivity of the piezoresistive characteristic. On the other hand, the piezoelectric sensor was accurate at high frequencies. Therefore, a full weight of one was given to w_{Pric} and the w_{Pive} was computed using (2). However, due to the harmonic measurements and zero strain axis crossing, the w_{Pive} and w_{Pric} values would approach infinity at these points. To mitigate this, ε_{act}, ε_{Pive} and ε_{Pric} were shifted in amplitude by a constant number c, which is a real positive number and assumed to be greater than twice of the maximum strain measurement's range. Then, w_{Pric} and w_{Pive} were computed using shifted data using (2) and (3). The final fused strain measurement is given by (4):

$$\varepsilon_f = w_{Pive} \times (\varepsilon_{Pive} + c) + w_{Pric} \times (\varepsilon_{Pric} + c) - c \tag{4}$$

In the fuzzy logic part of the fusion, the fusing process undergoes four consecutive stages to compute these weights. These stages are the fuzzification, rule generation, the FIS process, and defuzzification. Fuzzification is the processes of converting a crisp quantitative input to a fuzzy value that is conducted based on knowledge information [56]. The normalized measurement errors are fuzzified to span a range of values between zero and one using represented membership functions. The membership functions are labeled by linguistic variables representing the input or output information. The error membership functions fuzzified to span values of [0, 1] which maps the normalized inputs' errors. Either the piezoresistive weighting (w_{Pive}) or piezoelectric weighting (w_{Pric}) was selected to be FIS's output variables based on the characteristic sensitivity at specific operation frequency. Fuzzy Inference Systems (FIS) is the process of taking the fuzzy system's inputs into outputs based on the predetermined fuzzy rules. These rules are based on actual experimental data or knowledge-based. Defuzzification is the process of converting fuzzy value to a real quantity in contrast with the fuzzification process [56]. In the PPF method, the combined fuzzy output sets are defuzzified to achieve the w_{pive} or w_{pric} using the center of area (COA) method, which is recognized as the center of gravity, for Mamdani FIS type-1 [57], [58]. A weighted average is used to evaluate the output at type-1 Sugeno FIS [59].

In the study [41], the PVDF/MWNT strain sensor has been attached to a 28 cm Aluminum cantilever beam. The PNC sensor was attached at distance of 5 cm from the fixed end and vibration exciter was attached to the free end of the beam. The beam's width and thickness were 25 mm and 3 mm, respectively. Copper electrodes were attached to both end of the film, and double-sided tape was used to adhere the strain sensor to the cantilever. A commercial metal foil strain gauge was used for performance verification and comparison. A voltage divider was used to retrieve the piezoresistive measurement while a charge amplifier was used for piezoelectric characteristic. This study retrieved the MWCNT/PVDF piezoresistive and piezoelectric strain measurements in contrast to the reference strain gauge measurements, as shown in Fig. 2. The experimental data from [41] were used to generate and validate the PPF method using Fuzzy Logic and Global Optimization Toolboxes in MATLAB [60].

The actual strain is assumed to be equal to the strain gauge (reference) measurement data [41] in this study. Furthermore, the piezoresistive and piezoelectric data were used to develop and validate the proposed PPF method using the same data at the three different frequencies.

In this work, several approaches were used to achieve the PPF's FISs, which fuse both piezoresistive and piezoelectric characteristics. The FIS system contains several input and output membership functions and a set of rules that defines the input/output relationship. Designing and tuning such FIS for the PPF method is challenging process. As a result, data-driven based approaches were used for tuning FIS's parameters and learning the rules using the shifted data and weight values from (2) or (3). These approaches were the optimization method, data clustering, and combination of type-2 FIS and data clustering. These approaches are discussed in the following subsections. The constant value (c) of

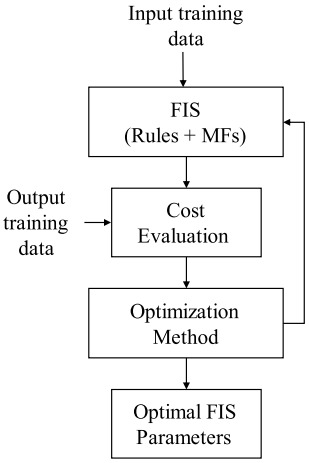

FIGURE 3. PPF's FIS tuning using data-driven optimization methods schematic.

0.001 was used for the fusion at 0.1 Hz while a constant value of one was used at 1 and 100 Hz frequencies.

A. OPTIMIZATION BASED PPF

The global optimization methods were implemented to develop the PPF's FIS at 0.1, 1, and 100 Hz strain measurements scenarios. The tuning process of the fuzzy system was conducted through two stages to improve the FIS's performance [61]. The first step was learning the rules of the fuzzy system using the given data. Then, tuning the parameters of both input and output membership functions (MFs) using the rules which were learned in the previous phase. As shown in Fig. 3, the optimization method adjusted the FIS's parameters given the cost of each solution which is the root mean square error (RMSE) in this study. The FIS retrieves the input training data and its output compared with the output training data to produce the solution's cost [61].

At frequencies 0.1 and 1 Hz, which considered a low frequencies strain measurements in this work, w_{Pive} was assigned a full weight of one and w_{Pric} was computed using equation (3) due to the high accuracy, sensitivity of piezoresistive characteristic. On the other hand, piezoelectric sensor is more accurate for strain measurement at high frequencies of 100 Hz, as shown in Fig. 2c. Therefore, a full weight of one was given to w_{Pric} and w_{Pive} was computed using (2). The normalized errors for both sensors and w_{Pric} were the inputs and output of the FISs; respectively, at the low frequencies. However, the w_{Pive} was considered the output for the FIS due to the high accuracy of piezoresistive sensor at high frequencies. The input and output data were divided into two data groups, training and validation data were using data with odd and even indexed sample number, respectively. Only training data were used to generate the PPF's FIS at different operation frequencies. Conversely, validation data were used to tune and verify the performance of FIS. In terms of optimization methods, particle swarm optimization was utilized at learning the rules phase under fixed input/output MFs' parameters using 20 iterations. The pattern search optimization method was used for tuning the FIS's parameters phase including rules and input/output MFs with 60 iterations. Three Gaussian MFs were chosen for the FIS's inputs and outputs at 0.1 and 100 Hz operation frequencies, while three MFs were used at 1 Hz.

B. DATA CLUSTERING BASED PPF

Data clustering is considered the foundation for many grouping and system modeling algorithms [62]. Clustering is the process of identifying and classifying a large set of data into common groups. These groups form a compact model that capture the system model's performance accurately. The Fuzzy Logic Toolbox^{TM}in MATLAB was used to identify the input/output data's clusters using strain measurement data at 0.1, 1, and 100 Hz frequencies. Two clustering approaches were used to develop the proposed PPF's FISs, which were fuzzy c-means (FCM) clustering and subtractive clustering. They are discussed in the following subsections.

1) FUZZY C-MEANS (FCM) CLUSTERING

The FCM clustering was presented by Jim Bezdek in 1981 [63]. In this technique, multidimensional data points fall into a group with certain degree of belongingness, controlled by a membership grade. The FCM command function in MATLAB was used to perform the FCM clustering for the input/output data sets and generate the PPF's FISs [64]. The FCM clustering process begins with initial random location of the cluster's centers and a membership grade specified for each data points. Each cluster's center is adjusted for data input/output set iteratively by updating the data point's cluster and membership grade. The distance between each data point and the cluster's center is the objective function which is to be minimized. The distance is weighted by the membership grade. The maximum number of iterations and minimum improvement between two consecutive iterations in the objective function's values were 100 and 1×10^{-5}, respectively. The number of clusters was chosen to be six for the PPF at 0.1 Hz and 100 Hz, while five clusters was used at 1 Hz data set classification. As a result, the number of input/outputs MFs and rules in the FIS equals number of specified cluster number for each frequency. The generated clusters' centers and membership grades were used by command line function *genfis* in MATLAB to develop a Mamdani-type FIS.

2) SUBTRACTIVE CLUSTERING

The subtractive clustering was introduced by Stephen Chiu in 1994 that significantly reduced the computational cost [65]. For any given input/output set of data, subtractive clustering is considered a quick way to estimate clusters' numbers and centers' locations. The *subclust* command function in MATLAB was used to perform the subtractive clustering for the data input/output sets and generate the PPF's FISs [66]. The subtractive cluster deals with each data point as possible cluster center. Depending on the distribution density of the input/output data points, the possibility of being a cluster center is calculated. The data point with highest likelihood is selected to be the first cluster's center, whereas

other number data points are removed based on the cluster influence range of the input/output clusters' centers. Then, the algorithm selects the following data point with the highest likelihood of being a cluster's center. The latter two steps are repeated until all data points fall inside the cluster influence range. A cluster influence range of one was used to produce the PPF's FISs at the three strain measurement frequencies. The generated clusters' centers were produced by command line function *genfis* in MATLAB to develop a Sugeno-type FIS. One rule was generated for each cluster, and one MF for input/output variables was produced for every cluster similar to the FCM clustering.

C. TYPE-2 FUZZY INFERENCE SYSTEM (FIS) BASED PPF

Previous PPF methods used the traditional type-1 MF, which has a unique membership value and utilizes a linguistic set to model the degree of membership [67]. However, type-1 MF does not include the model uncertainty in the membership's degree. On the other hand, type-2 MF has a range of values assign for the degree of membership. These values are ranging from upper membership function (UMF) and lower membership function (LMF), and the reign in between called the footprint of uncertainty (FOU). For the proposed PPF method, type-2 MF was utilized due to the model uncertainty that might arise during the KF model design for both piezoresistive and piezoelectric strain sensors.

The subtractive clustering was used in the input/output data set classification processes with cluster influence range of one. In addition, the command line function *genfis* in MATLAB was used to develop a Sugeno-type-1 FIS. The generated type-1 FISs were converted to type-2 FISs using *convertToType2* command line function [68]. The UMF of the generated type-2 FIS's parameters matched the MF of the type-1 FIS. The produced type-2 FIS utilizes default properties of the Karnik-Mendel (KM) reduction method to evaluate the output crisp value by finding the centroid of the type-2 fuzzy set [68], [69].

III. THE PPF METHOD TESTING AND VALIDATION MODEL

A Simulink model was constructed to validate the PPF method using the data in the study [41]. The model follows the schematic of the PPF method in Fig. 4 and calculates the final fused strain measurement using (4). The errors of both piezoresistive and piezoelectric sensors were computed and normalized. The normalized errors were fed to the fuzzy logic controller block which utilized the developed PPF's FISs for the frequencies 0.1, 1 and 100 Hz. The generated weight of w_{Pive} and w_{Pric} implemented in (4) beside the piezoresistive and piezoelectric strain measurement to evaluate the final fused strain measurements.

The final fused strain measurement was analyzed and investigated for their root mean square error (RMSE) with respect to the actual strain measurement. Additionally, it was compared with the optimal linear smoother based fusion technique at Park *et al.* study [41]. For the subtractive clustering based PPF, the generated weights were plotted for each frequency's scenario to evaluate the PPF method for their sensitivity and performance. The proposed PPF method fused both characteristics smoothly, taken the advantage of all available strain measurement data, and produced a sensitive wide band PVDF/MWNT strain sensor.

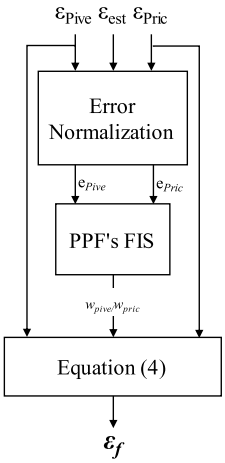

FIGURE 4. PPF's FIS testing and validating Simulink model's schematic.

IV. RESULTS AND DISCUSSIONS

The MWCNT/PVDF film has both piezoelectric and piezoresistive characteristics which strongly dependent on the dynamic loading frequency. The PPF method was analyzed at excitation frequencies of 0.1, 1, and 100 Hz. For strain measurement under small operational frequencies (0.1 Hz and 1 Hz), a full weight of one was given to the piezoresistive sensor due to the high sensitivity measurement. In addition, the PPF method predicted the piezoelectric's weight in the final fused signal based on the developed FISs. Whereas, the whole piezoelectric strain measurements were used due to their high accuracy and sensitivity at high frequency (100 Hz). The FISs were used to estimate the piezoresistive weight, which applied in the fusion process using (4). The performance of the resulted FISs, which based on optimization method, data clustering and fuzzy type-2 FIS, were validated and analyzed using fused strain's accuracy and RMSE. The generated subtractive based PPF's weights retrieved and investigated at the three frequencies. The following sections discusses the results of proposed PPF's performance.

A. OPTIMIZATION BASED PPF RESULTS

The optimization based PPF's FISs were tested for the operation frequencies 0.1, 1 and 100 Hz, as shown in Fig. 5. For the input/output labels, the piezoresistive and piezoelectric sensors' variables numbered as first and second, respectively. Each FIS has two input and output MFs except the FIS for 1 Hz operation frequency which has three MFs. The input variables' values span values between zero and one because the measurements' error for both sensors were normalized. The range of the MF's outputs were determined based on the maximum/minimum values of the estimated piezoresistive and piezoelectric's weights from either (2) or (3) at the three operation frequencies.

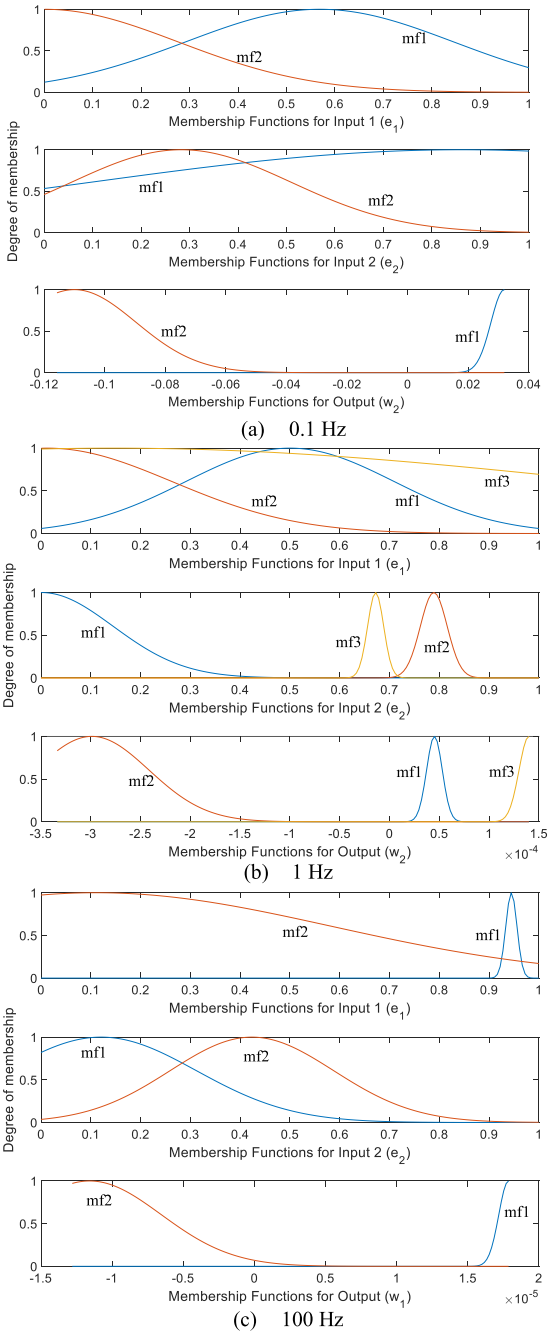

FIGURE 5. Input and output MFs of optimization based PPF's FISs.

The developed FIS conveyed fuzzy system's inputs into the desired outputs based on the predetermined fuzzy rules. The final set of rules were generated from the tuning stage using *tunefis* command line function, as shown in Table 1. These rules governed the relationship between the FIS's inputs and produces the desired outputs. The number of generated rules for the three operation frequencies 0.1, 1, 100 Hz were 5, 11, and 5, respectively. A higher number of rules was associated with the 1 Hz FIS due to the higher number of MFs need to relate to each other and the desire weight. To connect between the antecedent's conditions, AND (&) operator, which stands for the minimum value among these

TABLE 1. Optimization based PPF's FISs rules.

Frequency	FIS's rules
0.1 Hz	1. If (en1 is mf2) and (en2 is mf2) then (w2 is mf2) (1) 2. If (en1 is mf1) and (en2 is mf1) then (w2 is mf1) (1) 3. If (en1 is mf1) and (en2 is mf2) then (w2 is mf1) (1) 4. If (en1 is mf2) and (en2 is mf1) then (w2 is mf2) (1) 5. If (en1 is mf2) then (w2 is mf2) (1)
1 Hz	1. If (en1 is mf1) then (w2 is mf3) (1) 2. If (en1 is mf2) and (en2 is mf1) then (w2 is mf2) (1) 3. If (en2 is mf3) then (w2 is mf1) (1) 4. If (en2 is mf2) then (w2 is mf1) (1) 5. If (en1 is mf3) and (en2 is mf3) then (w2 is mf1) (1) 6. If (en1 is mf1) and (en2 is mf3) then (w2 is mf1) (1) 7. If (en1 is mf1) and (en2 is mf1) then (w2 is mf3) (1) 8. If (en1 is mf2) and (en2 is mf2) then (w2 is mf2) (1) 9. If (en1 is mf2) and (en2 is mf3) then (w2 is mf1) (1) 10. If (en1 is mf3) and (en2 is mf2) then (w2 is mf1) (1) 11. If (en1 is mf2) then (w2 is mf2) (1)
100 Hz	1. If (en1 is mf1) and (en2 is mf2) then (w1 is mf1) (1) 2. If (en2 is mf2) then (w1 is mf1) (1) 3. If (en2 is mf1) then (w1 is mf2) (1) 4. If (en1 is mf2) and (en2 is mf1) then (w1 is mf2) (1) 5. If (en1 is mf2) and (en2 is mf2) then (w1 is mf1) (1)

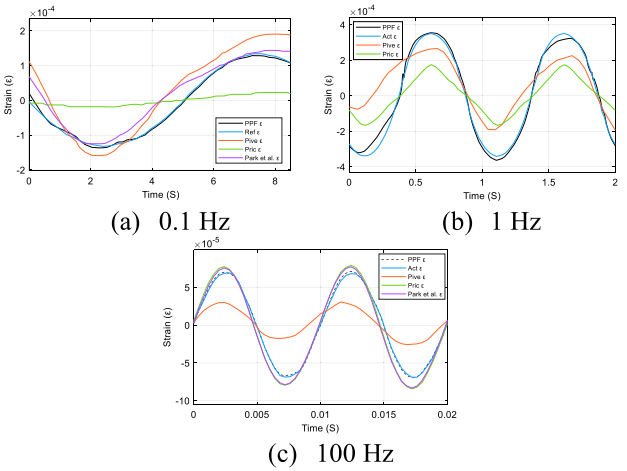

FIGURE 6. Optimization based PPF FISs' fused output strain.

conditions' values, was used. The Min implication method was implemented to achieve the proposed FISs. In addition, the MAX method of aggregation was utilized to combine the rule's outputs into a solo fuzzy set. The center of area (COA) was used to defuzzifying the combined fuzzy's output sets in order to generate the appropriate sensors' weights.

The estimated fused strain was generated and compared with the actual, piezoresistive and piezoelectric strain sensors at the three different frequencies, as shown in Fig. 6. A good agreement between the actual strain measurements and the PPF's fused strains is observed using the optimization based FISs. This accuracy achieved with comparable low iteration numbers, where 20 and 60 iterations were used for learning and tuning the FISs's rules and parameters, respectively.

B. CLUSTERING BASED PPF RESULTS

The fusion FISs based on the two data clustering methods were retrieved and verified at the operating frequencies of 0.1, 1 and 100 Hz. The clustering methods used were the

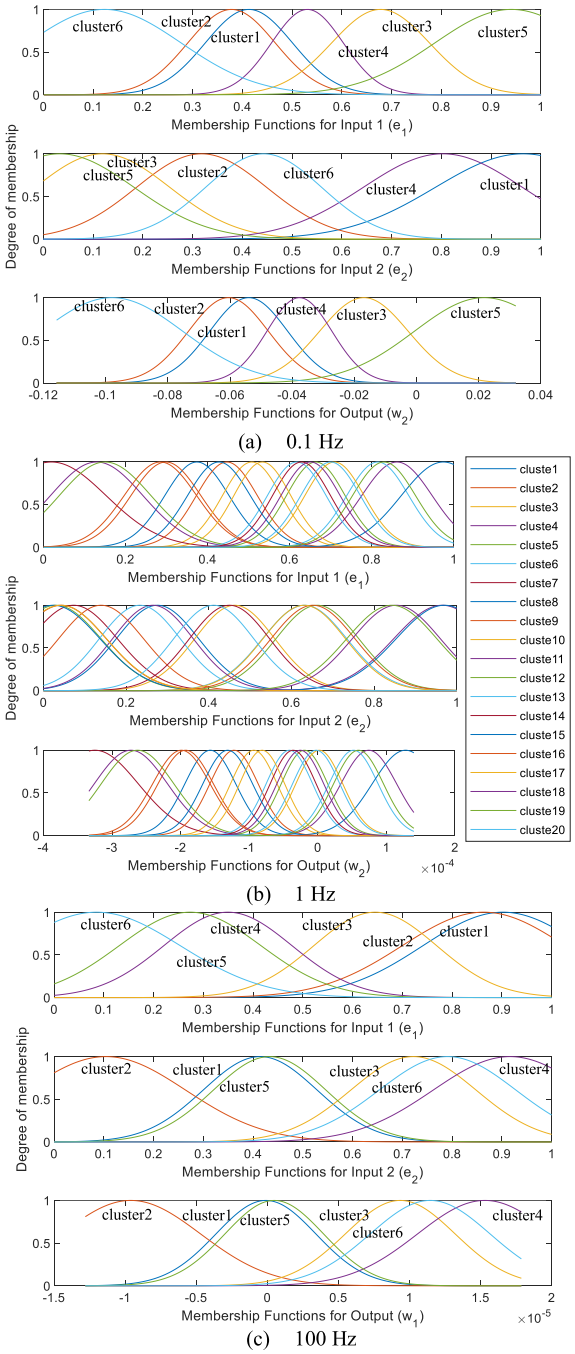

FIGURE 7. Input and output MFs of FCM based PPF's FISs.

FCM and subtractive clustering. The FISs were analyzed for their input/output MFs' parameter, generated rules and fused strain's RMSE in the following subsections.

1) FUZZY C-MEANS CLUSTERING (FCM) CLUSTERING

As shown in Fig. 7, the MFs for input/output variables were generated to fuse the piezoresistive and piezoelectric NC sensors at the three-operation frequency. The ranges of both input and output variables matched those used in the optimization-based FIS. A minimum number of MFs, which could achieve good and accurate fused strain, was

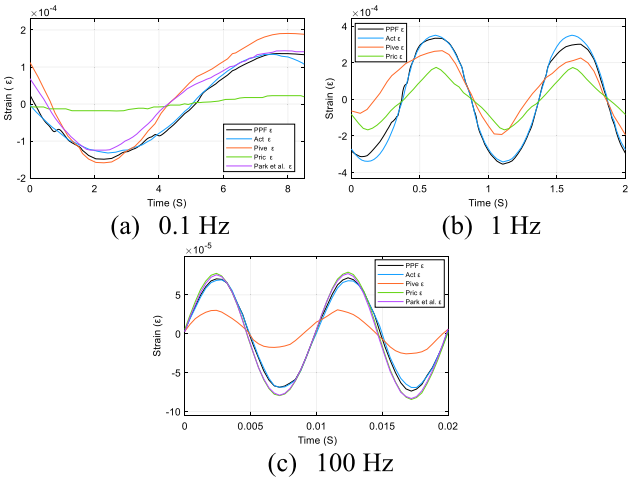

FIGURE 8. FCM clustering based PPF FISs' fused output strain.

defined manually. As shown in Fig.7a and 7c, the number of input/output's MFs have been chosen to be six MFs at 0.1 Hz and 100 Hz, while 20 MFs was chosen for the strain measurements fusion at 100 Hz, as shown in Fig.7b. The piezoresistive and piezoelectric characteristic had relatively higher error at the 100 Hz compared to other operation frequencies as shown in Fig. 2b. However, minimizing the MFs would reduce the output computation complexity and decrease the fused strain accuracy. The MFs were labeled by variables representing the cluster number for input/output variables' values.

A set of rules was produced for the FCM clustering based FIS using the *genfis* command line function, as shown in Table 2. The FISs for 0.1 and 100 Hz frequencies shared six generated rules. While 20 rules were assigned for the 1 Hz fusion frequency. The number of MFs and rules associated with each frequency were equal. The AND (&) operator was used to connect between the antecedent's conditions and MIN implication method was implemented to achieve the proposed FISs. Additionally, the MAX method of aggregation was utilized to combine the rule's outputs into a solo fuzzy set. To generate the appropriate sensors weights for the proposed Mamdani FIS, the COA was used to defuzzifying the combined fuzzy's output similar to the optimization based FISs.

As shown in Fig. 8, the performance of the generated FISs using the FCM clustering was evaluated. Compared to the piezoresistive and piezoelectric strain sensors at the three different frequencies, the PPF method had a good agreement with the actual strain, which measured using the strain gauge. The FIS at 1 Hz mismatched the three peaks out four, but still more accurate the piezoresistive and piezoelectric sensors. The fusion at 100 Hz achieved higher accuracy compared two other FCM based FISs. Compared to the Park *et al.* fusion at 0.1 Hz and 100 Hz, the PPF's fused strains matched well with the actual strain despite the higher number input/output MFs.

2) SUBTRACTIVE CLUSTERING

The subtractive clustering was the second approach that based on data classification. A Sugeno based FIS, which utilize

TABLE 2. FCM Clustering based PPF's FISs rules.

Frequency	FIS's rules
0.1 Hz and 100 Hz	1. If (in1 is in1cluster1) and (in2 is in2cluster1) then (out1 is out1cluster1) (1) 2. If (in1 is in1cluster2) and (in2 is in2cluster2) then (out1 is out1cluster2) (1) 3. If (in1 is in1cluster3) and (in2 is in2cluster3) then (out1 is out1cluster3) (1) 4. If (in1 is in1cluster4) and (in2 is in2cluster4) then (out1 is out1cluster4) (1) 5. If (in1 is in1cluster5) and (in2 is in2cluster5) then (out1 is out1cluster5) (1) 6. If (in1 is in1cluster6) and (in2 is in2cluster6) then (out1 is out1cluster6) (1)
1 Hz	1. If (in1 is in1cluster1) and (in2 is in2cluster1) then (out1 is out1cluster1) (1) 2. If (in1 is in1cluster2) and (in2 is in2cluster2) then (out1 is out1cluster2) (1) *n*. If (in1 is in1cluster *n*) and (in2 is in2cluster *n*) then (out1 is out1cluster *n*) (1) … Where *n*= 1, 2,…, 20 … 20. If (in1 is in1cluster20) and (in2 is in2cluster20) then (out1 is out1cluster20) (1)

singleton output MFs, was used to develop the PPF's FIS [70]. The output MFs can be in the form of either a constant or linear function in terms of the input values. The linear function based Sugeno FIS was used for this study. The final output weight is computed using the i rule output level (z_i) and rule firing strength (w_i). The z_i is function in two inputs values e_1 and e_2 and three constant values a_i, b_i and c_i, which generated using *genfis* command line function in MATLAB, as shown in (5):

$$z_i = a_i x + b_i y + c_i \tag{5}$$

where w_i is evaluated from the rule antecedent using AND method for both input errors. The weighted average was used to compute final output weigh for N number of rules, as follow (6):

$$Final\ Output\ Weight = \frac{\sum_{i=1}^{N} w_i z_i}{\sum_{i=1}^{N} w_i} \tag{6}$$

The FISs input's MFs and output linear equations' constants were generated and tuned using subtractive clustering technique, as shown in Fig. 9. Two MFs were assigned for the normalized error inputs at the three strain measurement frequencies. Each MF represented a cluster of range of input values. The z_i functions associated with the piezoelectric output weight at 0.1 Hz and 1 Hz frequencies while piezoresistive output weight at 100 Hz. The constant values of each FIS were retrieved to evaluate the final output weights using the weighting average.

Set of FISs' rules were generated from the subtractive clustering process using the *genfis* command line function, as shown in Table 3. Similar to the MFs' number, three rules were produced for the FISs at 0.1 and 100 Hz frequencies. The AND (&) operator was used to combine the fuzzified input's values for each rule. To generate the appropriate

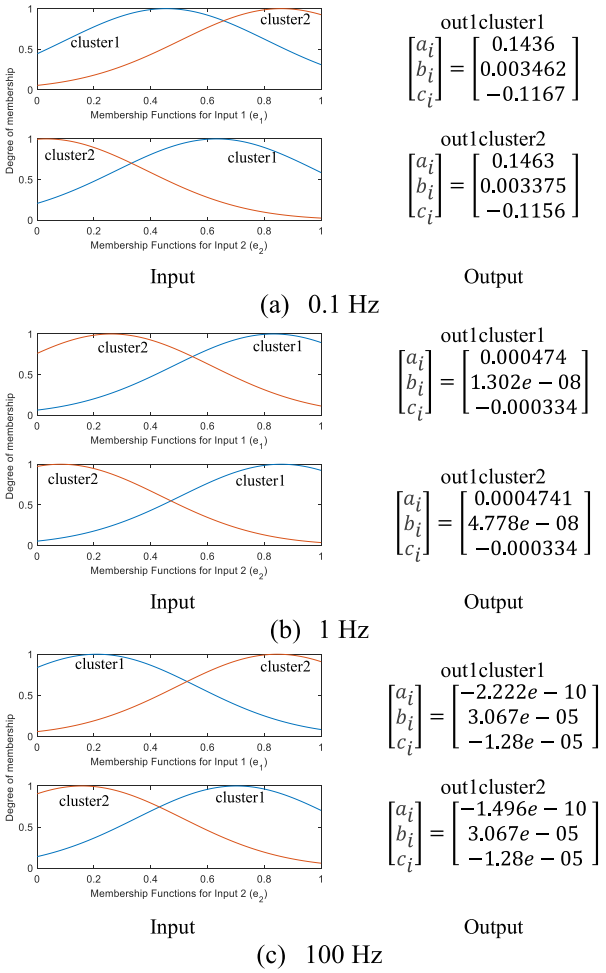

FIGURE 9. Input and output MFs of Subtractive clustering based PPF's FISs.

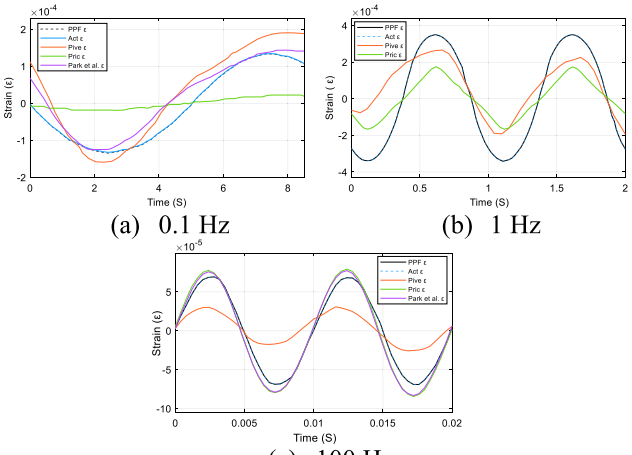

FIGURE 10. Subtractive clustering based PPF's FISs output fused strain.

sensors weights, the weighting average was used. The AND operator works as a product of fuzzified input values [59]. This clustering method generate multi-label two MFs FISs that has the same set of rules. The differences between the developed subtractive based FISs were the input MFs' parameters and the output linear function constants' values.

TABLE 3. Subtractive clustering based PPF's FISs rules.

Frequency	FIS's rules
0.1 Hz 1 Hz 100 Hz	1. If (in1 is in1cluster1) and (in2 is in2cluster1) then (out1 is out1cluster1) (1) 2. If (in1 is in1cluster2) and (in2 is in2cluster2) then (out1 is out1cluster2) (1)

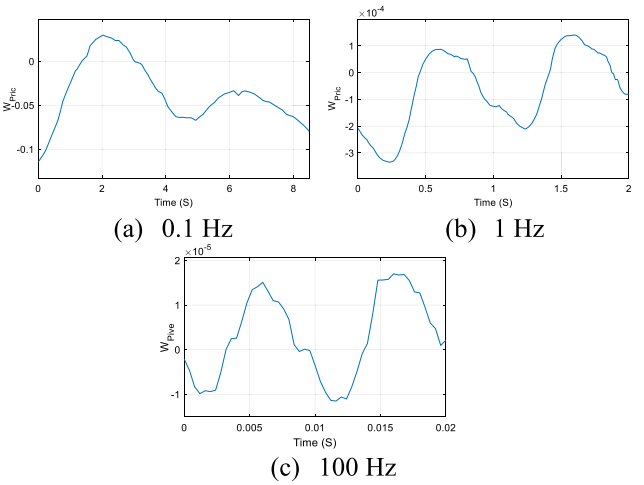

FIGURE 11. Subtractive clustering based PPF's FISs output weights.

The subtractive based PPF fusion method was tested and compared with the NC piezoresistive and piezoelectric strain signals, as shown in Fig. 10. A very good agreement between the actual strain measurements and the PPF's fused strains was achieved using the subtractive clustering based FISs compare to the Park *et al.* fusions at 0.1 Hz and 100 Hz. A distinguished performance was achieved using comparable small number of MFs, where only two MFs were utilized for the three operation frequencies compared to previous methods.

The piezoresistive and piezoelectric weights were retrieved to analyze the developed subtractive based PPF method, as shown in Fig. 11. Higher piezoelectric weights were generated by the PPF method at 1 Hz compared to 0.1 Hz and the piezoresistive weights at 100 Hz, as shown in Fig. 11b. It is due to the higher error of both piezoresistive and piezoelectric sensors with respect of the actual strain measurements. Conversely, the generated piezoresistive's weights at 100 Hz were relatively small, as shown in Fig. 11c. It was influenced by the approximately harmonic error shape and comparatively accurate piezoelectric strain sensor. Capturing the error signals' shapes using fuzzy system had great impact on the PPF method.

C. TYPE-2 FUZZY INFERENCE SYSTEM PPF

Type-1 fuzzy input MFs was used to model the degree of membership for input values within a fuzzy set or cluster in the previous methods. However, it does not incorporate the model uncertainty in the membership's degree. As a result, the subtractive based FISs, which were developed in the previous subsection, were converted to type-2 FISs, as shown in Fig. 12. The input MFs were type-2 fuzzy set, while the

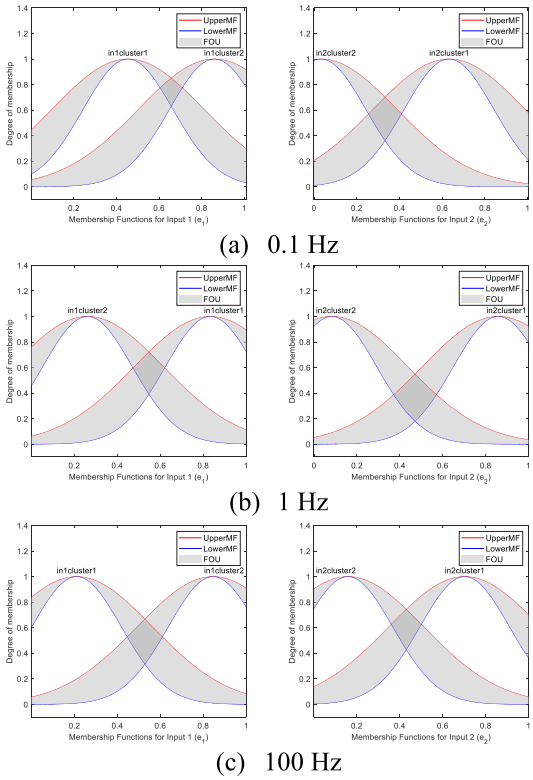

FIGURE 12. Input and output MFs of fuzzy type-2 based PPF's FISs.

type-1 Sugeno system output MFs were kept the same. Each input membership function consists of upper MF (UMF) and lower MF (LMF), where the upper MF matches the type-1 MF. The footprint of uncertainty spans the region between the upper and lower MFs.

As shown in Table 3, the subtractive clustering-based FIS's rules were used for the type-2 FIS' fusion. Total number of two rules were generated and matched the number of MFs. Unlike the type-1 Sugeno system, the degree of membership for LMFs and UMFs were retrieved to fuzzified the inputs' values. As a result, each MF had two fuzzy values and the AND (&) operator was used to combine the fuzzified input's values for each rule resulting in a range of rule firing strength [71]. To evaluate the output crisp value, the aggregated type-2 fuzzy set converted to type-1 fuzzy set, which called the centroid of the type-2 fuzzy set. The KM reduction method was used to iteratively evaluate the centroid [69].

The fuzzy type-2 PPF fusion method was tested and compared with the piezoresistive and piezoelectric strain sensors, as shown in Fig. 13. Similar to the subtractive based fusion, high agreement between the actual strain measurements and the PPF's fused strains when compared to the Park *et al.* fusion method at 0.1 Hz and 100 Hz. This performance was accomplished using only two MFs for the three operation frequencies.

The RMSE of the developed PPF's FISs were computed, analyzed and compared with the Park *et al.* fusion method, as shown in Fig. 14. Using the optimization methods, the smallest PPF fused strains' RMSE was

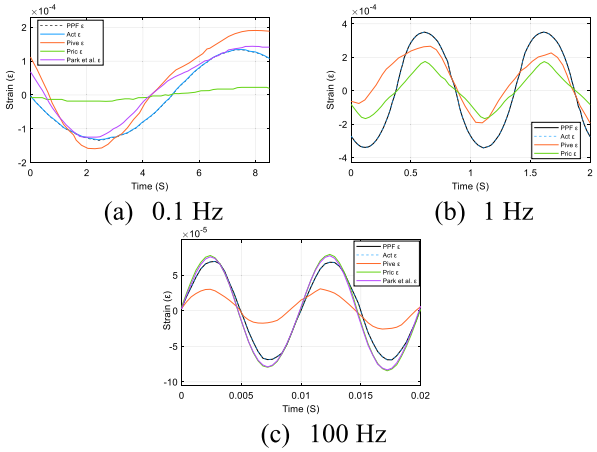

FIGURE 13. Fuzzy type-2 based PPF's FISs output fused strain's error.

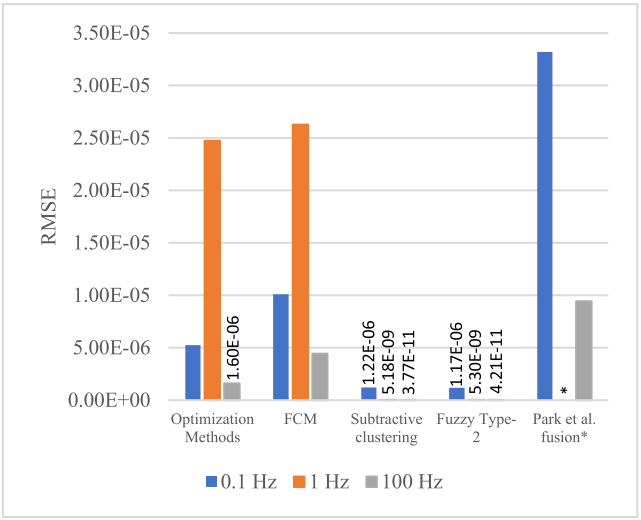

* Fusion at 1 Hz is not provided in the study Park at el. [41].

FIGURE 14. Fused strain's RMSE using PPF's FISs at different frequencies and compared with Park at el. fusion's RMSE.

recorded as 1.596E-06 at 100 Hz. The maximum RMSE of 2.475E-05 accrued at the 1 Hz strain fusion. The fused strain using the proposed PPF method minimized the RMSE significantly compared to the Park *et al.* fusion method. The fusion at 1 Hz was not provided in the study [41] to compare with current fusion method. For the FCM based PPF, the smallest RMSE of 4.43E-06 was calculated at 100 Hz using the PPF method. Compared to the Park *et al.* fusion method, the proposed PPF method obtained accurate fused strain measurements. The smallest RMSE of 5.18E-09 and 3.77E-11 were found at 1 Hz and 100 Hz; respectively, using the subtractive clustering based PPF method. At 1 Hz, the RMSE was found to be to be 2.628E-05, approximately similar to the RMSE of the optimization-based FIS. Both the FCM and optimization based FISs based on Mamdani FIS, which does not overcome the Sugeno FIS in the nonlinear dynamic application. On the contrary, the PPF successfully estimated the fused strain at 1 Hz and 100 Hz using the subtractive clustering and fuzzy type-2 based methods. An average RMSE of 2.64E-09 was estimated at these frequencies. In addition, at very low frequency strain measurement fusion of 0.1 Hz, both clusters based PPF fusion minimize the RMSE compared to the Park *et al.* fusion. Combining the subtractive clustering with type-2 FIS resulted in reducing the RMSE by approximately 4%. This improvement gained by the model uncertainty feature of the fuzzy type-2 PPF. The developed PPF's FISs, based on type-2 fuzzy method, successfully fused the piezoresistive and piezoelectric measurements and produce accurate fused strain measurements.

The results of this study indicate that a real time wide band nanocomposite strain sensor can be achieved using the proposed PPF method. The subtractive based PPF utilized the smallest number of two MFs in the three operation frequencies to perform the fusion which minimize the computation time for real time strain measurements fusion. Similarly, the optimization based PPF fused both MWCNT/PVDF measurement's characteristics and had the same number of MFs at 0.1 Hz and 100 Hz with relatively higher RMSEs. The fuzzy type-2 and subtractive had the same number of two MFs and approximately similar RMSE. The FCM clustering based PPF contained the highest number MFs, which were 20 and 6 MFs, compare to the other derived FISs. The PPF successfully fused the piezoresistive and piezoelectric characteristics at their optimal performance and sensitivity. In the current study, the estimate of actual strain measurements was assumed to be available.

V. CONCLUSION

The *In situ* MWCNT/PVDF nanocomposite strain senor has potential to capture both low and high frequency dynamic strain measurements using both piezoresistive and piezoelectric measurements, respectively. However, the band frequencies of the strain sensor are limited to either piezoresistive or piezoelectric depending on the design or measurements criteria. In this study, a novel PPF method is proposed that effectively combined both piezoresistive and piezoelectric characteristics to capture wide frequency MWCNT/PVDF strain measurements in real time. The proposed piezoresistive/piezoelectric fusion (PPF), which is based on a fuzzy logic inference engine, was introduced to combine both piezoresistive and piezoelectric sensor data.

Different technique and methods were used to generate the PPF's FISs, such as optimization method, data clustering and fuzzy type-2 system using MATLAB. The FCM clustering, subtractive clustering, and type-2 FISs were investigated and compared with other fusion method in the literature. At low frequency (0.1 Hz and 1 Hz) strain measurement, the piezoresistive sensor was assigned a full weight while the PPF's FISs estimate the necessary piezoelectric contribution weight. Both weights beside the piezoresistive and piezoelectric strain measurements were used to enhance the frequency range and increase measurements accuracy using the developed fusion equation. The subtractive cluster and type-2 FIS based PPF fused both measurements while attaining high accuracy and relatively small RMSEs. However,

type-2 FIS based PPF reduced the subtractive clustering's RMSE by approximately 4% at the frequency 0.1 Hz by including the footprint of uncertainty. Both methods were able to fuse the measurement using Sugeno FIS using only two MFs for input/output variables. The optimization-based FIS, with maximum number of MFs of three, utilized the particle swarm optimization and pattern search algorithms to learn and tune the FIS's parameters, respectively. Additionally, the optimization based FISs's RMSE was approximately 60.47 % less than the FCM based FISs among the three frequency. Sugeno based PPF indicated high accuracy compared to the Mamdani FIS because of the Sugeno ability to work with dynamic nonlinear systems efficiently. The developed PPF was verified with experimental data at different dynamic frequencies presented in [41]. The results correlated very well with the actual strain measurement and greatly reduced measurement error of both characteristics. The proposed fusion approach has the potential for other measurement methods, which are influenced by input frequency or similar environment.

A more rigorous experimental validation of the proposed fusion method is currently underway. However, future work needs to concentrate on constructing a KF or equivalent circuit model, which will simulate the MWCNT/PVDF strain sensors' characteristics. These models should capture the frequency dependent performance characteristics with an actual strain estimate. The estimated error would be employed by the PPF method for optimal fused strain measurement estimates. On a wider level, the PPF could be applied to different sensing applications, where frequency or other phenomenon influencing their performance could be improved through this fusion based estimate overcoming such limitations.

REFERENCES

[1] Z. Lou, H. Han, M. Zhou, J. Wan, Q. Sun, X. Zhou, and N. Gu, "Fabrication of magnetic conjugation clusters via intermolecular assembling for ultrasensitive surface plasmon resonance (SPR) detection in a wide range of concentrations," *Anal. Chem.*, vol. 89, no. 24, pp. 13472–13479, Dec. 2017.

[2] J. Zhou, T. Yang, J. Chen, C. Wang, H. Zhang, and Y. Shao, "Two-dimensional nanomaterial-based plasmonic sensing applications: Advances and challenges," *Coordination Chem. Rev.*, vol. 410, May 2020, Art. no. 213218, doi: 10.1016/j.ccr.2020.213218.

[3] C. Gau, H. S. Ko, and H. T. Chen, "Piezoresistive characteristics of MWNT nanocomposites and fabrication as a polymer pressure sensor," *Nanotechnology*, vol. 20, no. 18, May 2009, Art. no. 185503, doi: 10.1088/0957-4484/20/18/185503.

[4] S. Borovik and Y. Sekisov, "Single-coil eddy current sensors and their application for monitoring the dangerous states of gas-turbine engines," *Sensors*, vol. 20, no. 7, p. 2107, Apr. 2020, doi: 10.3390/s20072107.

[5] C.-Y. Lin, Y.-Y. Fang, C.-W. Lin, J. J. Tunney, and K.-C. Ho, "Fabrication of NO_x gas sensors using In_2O_3–ZnO composite films," *Sens. Actuators B, Chem.*, vol. 146, no. 1, pp. 28–34, Apr. 2010, doi: 10.1016/j.snb.2010.02.040.

[6] B. Mitchell, J. Koo, I. Iordachita, P. Kazanzides, A. Kapoor, J. Handa, G. Hager, and R. Taylor, "Development and application of a new steady-hand manipulator for retinal surgery," in *Proc. IEEE Int. Conf. Robot. Autom.*, Apr. 2007, pp. 623–629.

[7] Y. Kakinuma, K. Igarashi, S. Katsura, and T. Aoyama, "Development of 5-axis polishing machine capable of simultaneous trajectory, posture, and force control," *CIRP Ann.*, vol. 62, no. 1, pp. 379–382, 2013, doi: 10.1016/j.cirp.2013.03.135.

[8] R. A. Brookhuis, T. S. J. Lammerink, R. J. Wiegerink, M. J. de Boer, and M. C. Elwenspoek, "3D force sensor for biomechanical applications," *Sens. Actuators A, Phys.*, vol. 182, pp. 28–33, Aug. 2012, doi: 10.1016/j.sna.2012.04.035.

[9] D. Trivedi, C. D. Rahn, W. M. Kier, and I. D. Walker, "Soft robotics: Biological inspiration, state of the art, and future research," *Appl. Bionics Biomech.*, vol. 5, no. 3, pp. 99–117, Dec. 2008, doi: 10.1080/11762320802557865.

[10] P. Estevez, J. M. Bank, M. Porta, J. Wei, P. M. Sarro, M. Tichem, and U. Staufer, "6 DOF force and torque sensor for micro-manipulation applications," *Sens. Actuators A, Phys.*, vol. 186, pp. 86–93, Oct. 2012, doi: 10.1016/j.sna.2012.02.037.

[11] A. M. Alotaibi, S. Anwar, M. T. Loghmani, and S. Chien, "Force sensing for an instrument-assisted soft tissue manipulation device," *J. Med. Devices*, vol. 11, no. 3, Sep. 2017, Art. no. 031012, doi: 10.1115/1.4036654.

[12] S. Iijima, "Helical microtubules of graphitic carbon," *Nature*, vol. 354, no. 6348, pp. 56–58, Nov. 1991, doi: 10.1038/354056a0.

[13] J.-P. Salvetat, J.-M. Bonard, N. H. Thomson, A. J. Kulik, L. Forró, W. Benoit, and L. Zuppiroli, "Mechanical properties of carbon nanotubes," *Appl. Phys. A, Solids Surf.*, vol. 69, no. 3, pp. 255–260, Sep. 1999, doi: 10.1007/s003390050999.

[14] R. S. Ruoff and D. C. Lorents, "Mechanical and thermal properties of carbon nanotubes," *Carbon*, vol. 33, no. 7, pp. 925–930, 1995, doi: 10.1016/0008-6223(95)00021-5.

[15] K. Yoshino, H. Kajii, H. Araki, T. Sonoda, H. Take, and S. Lee, "Electrical and optical properties of conducting polymer—Fullerene and conducting polymer—Carbon nanotube composites," *Fullerene Sci. Technol.*, vol. 7, no. 4, pp. 695–711, Jul. 1999, doi: 10.1080/10641229909351371.

[16] Z. Yao, C. L. Kane, and C. Dekker, "High-field electrical transport in single-wall carbon nanotubes," *Phys. Rev. Lett.*, vol. 84, no. 13, pp. 2941–2944, Mar. 2000, doi: 10.1103/physrevlett.84.2941.

[17] P. Kim, L. Shi, A. Majumdar, and P. L. McEuen, "Thermal transport measurements of individual multiwalled nanotubes," *Phys. Rev. Lett.*, vol. 87, no. 21, 2001, Art. no. 215502, doi: 10.1103/physrevlett.87.215502.

[18] C. Yu, L. Shi, Z. Yao, D. Li, and A. Majumdar, "Thermal conductance and thermopower of an individual single-wall carbon nanotube," *Nano Lett.*, vol. 5, no. 9, pp. 1842–1846, Sep. 2005, doi: 10.1021/nl051044e.

[19] J. K. W. Sandler, J. E. Kirk, I. A. Kinloch, M. S. P. Shaffer, and A. H. Windle, "Ultra-low electrical percolation threshold in carbon-nanotube-epoxy composites," *Polymer*, vol. 44, no. 19, pp. 5893–5899, Sep. 2003, doi: 10.1016/s0032-3861(03)00539-1.

[20] K. Kalaitzidou, H. Fukushima, and L. T. Drzal, "A new compounding method for exfoliated graphite–polypropylene nanocomposites with enhanced flexural properties and lower percolation threshold," *Compos. Sci. Technol.*, vol. 67, no. 10, pp. 2045–2051, Aug. 2007, doi: 10.1016/j.compscitech.2006.11.014.

[21] A. Celzard, E. McRae, C. Deleuze, M. Dufort, G. Furdin, and J. F. Marêché, "Critical concentration in percolating systems containing a high-aspect-ratio filler," *Phys. Rev. B, Condens. Matter*, vol. 53, no. 10, pp. 6209–6214, Mar. 1996, doi: 10.1103/physrevb.53.6209.

[22] S. H. Munson-McGee, "Estimation of the critical concentration in an anisotropic percolation network," *Phys. Rev. B, Condens. Matter*, vol. 43, no. 4, pp. 3331–3336, Feb. 1991, doi: 10.1103/physrevb.43.3331.

[23] I. Alig, P. Pötschke, D. Lellinger, T. Skipa, S. Pegel, G. R. Kasaliwal, and T. Villmow, "Establishment, morphology and properties of carbon nanotube networks in polymer melts," *Polymer*, vol. 53, no. 1, pp. 4–28, Jan. 2012, doi: 10.1016/j.polymer.2011.10.063.

[24] M. Moniruzzaman and K. I. Winey, "Polymer nanocomposites containing carbon nanotubes," *Macromolecules*, vol. 39, no. 16, pp. 5194–5205, Aug. 2006, doi: 10.1021/ma060733p.

[25] Alamusi, N. Hu, H. Fukunaga, S. Atobe, Y. Liu, and J. Li, "Piezoresistive strain sensors made from carbon nanotubes based polymer nanocomposites," *Sensors*, vol. 11, no. 11, pp. 10691–10723, Nov. 2011, doi: 10.3390/s111110691.

[26] B. Hu, N. Hu, Y. Li, K. Akagi, W. Yuan, T. Watanabe, and Y. Cai, "Multi-scale numerical simulations on piezoresistivity of CNT/polymer nanocomposites," *Nanosc. Res. Lett.*, vol. 7, no. 1, p. 402, Dec. 2012, doi: 10.1186/1556-276x-7-402.

[27] C. Li, E. T. Thostenson, and T.-W. Chou, "Dominant role of tunneling resistance in the electrical conductivity of carbon nanotube–based composites," *Appl. Phys. Lett.*, vol. 91, no. 22, Nov. 2007, Art. no. 223114, doi: 10.1063/1.2819690.

[28] A. V. Shirinov and W. K. Schomburg, "Pressure sensor from a PVDF film," *Sens. Actuators A, Phys.*, vol. 142, no. 1, pp. 48–55, Mar. 2008, doi: 10.1016/j.sna.2007.04.002.
[29] R. Pérez, M. Král, and H. Bleuler, "Study of polyvinylidene fluoride (PVDF) based bimorph actuators for laser scanning actuation at kHz frequency range," *Sens. Actuators A, Phys.*, vol. 183, pp. 84–94, Aug. 2012, doi: 10.1016/j.sna.2012.05.019.
[30] V. T. Rathod, D. R. Mahapatra, A. Jain, and A. Gayathri, "Characterization of a large-area PVDF thin film for electro-mechanical and ultrasonic sensing applications," *Sens. Actuators A, Phys.*, vol. 163, no. 1, pp. 164–171, Sep. 2010, doi: 10.1016/j.sna.2010.08.017.
[31] A. Glück, W. Halder, G. Lindner, H. Müller, and P. Weindler, "PVDF-excited resonance sensors for gas flow and humidity measurements," *Sens. Actuators B, Chem.*, vol. 19, nos. 1–3, pp. 554–557, Apr. 1994, doi: 10.1016/0925-4005(93)01083-g.
[32] J. Xu, M. J. Dapino, D. Gallego-Perez, and D. Hansford, "Microphone based on polyvinylidene fluoride (PVDF) micro-pillars and patterned electrodes," *Sens. Actuators A, Phys.*, vol. 153, no. 1, pp. 24–32, Jun. 2009, doi: 10.1016/j.sna.2009.04.008.
[33] C. J. Sielmann, J. R. Busch, B. Stoeber, and K. Walus, "Inkjet printed all-polymer flexural plate wave sensors," *IEEE Sensors J.*, vol. 13, no. 10, pp. 4005–4013, Oct. 2013, doi: 10.1109/jsen.2013.2264930.
[34] D. Vatansever, R. L. Hadimani, T. Shah, and E. Siores, "An investigation of energy harvesting from renewable sources with PVDF and PZT," *Smart Mater. Struct.*, vol. 20, no. 5, May 2011, Art. no. 055019, doi: 10.1088/0964-1726/20/5/055019.
[35] A. Ramaratnam and N. Jalili, "Reinforcement of piezoelectric polymers with carbon nanotubes: Pathway to next-generation sensors," *J. Intell. Mater. Syst. Struct.*, vol. 17, no. 3, pp. 199–208, Mar. 2006, doi: 10.1177/1045389x06055282.
[36] J. Kim, K. J. Loh, and J. P. Lynch, "Piezoelectric polymeric thin films tuned by carbon nanotube fillers," *Proc. SPIE*, vol. 6932, Mar. 2008, Art. no. 693232.
[37] J. S. Lee, G. H. Kim, W. N. Kim, K. H. Oh, H. T. Kim, S. S. Hwang, and S. M. Hong, "Crystal structure and ferroelectric properties of poly (vinylidene fluoride)-carbon nano tube nanocomposite film," *Mol. Cryst. Liq. Cryst.*, vol. 491, no. 1, pp. 247–254, Sep. 2008, doi: 10.1080/15421400802330861.
[38] Z. Zeng, M. Liu, H. Xu, Y. Liao, F. Duan, L.-M. Zhou, H. Jin, Z. Zhang, and Z. Su, "Ultra-broadband frequency responsive sensor based on lightweight and flexible carbon nanostructured polymeric nanocomposites," *Carbon*, vol. 121, pp. 490–501, Sep. 2017, doi: 10.1016/j.carbon.2017.06.011.
[39] Y. Liao, F. Duan, H. Zhang, Y. Lu, Z. Zeng, M. Liu, H. Xu, C. Gao, L.-M. Zhou, H. Jin, Z. Zhang, and Z. Su, "Ultrafast response of spray-on nanocomposite piezoresistive sensors to broadband ultrasound," *Carbon*, vol. 143, pp. 743–751, Mar. 2019, doi: 10.1016/j.carbon.2018.11.074.
[40] C.-M. Wu, M.-H. Chou, and W.-Y. Zeng, "Piezoelectric response of aligned electrospun polyvinylidene fluoride/carbon nanotube nanofibrous membranes," *Nanomaterials*, vol. 8, no. 6, p. 420, Jun. 2018, doi: 10.3390/nano8060420.
[41] M. Sanati, A. Sandwell, H. Mostaghimi, and S. Park, "Development of nanocomposite-based strain sensor with piezoelectric and piezoresistive properties," *Sensors*, vol. 18, no. 11, p. 3789, Nov. 2018, doi: 10.3390/s18113789.
[42] K. Ke, Y. Wang, K. Zhang, Y. Luo, W. Yang, B.-H. Xie, and M.-B. Yang, "Melt viscoelasticity, electrical conductivity, and crystallization of PVDF/MWCNT composites: Effect of the dispersion of MWCNTs," *J. Appl. Polym. Sci.*, vol. 125, no. S1, pp. E49–E57, Jul. 2012, doi: 10.1002/app.36293.
[43] M. Han, Y. C. Chan, W. Liu, S. Zhang, and H. Zhang, "Low frequency PVDF piezoelectric energy harvester with combined d31 and d33 operating modes," in *Proc. 8th Annu. IEEE Int. Conf. Nano/Micro Eng. Mol. Syst.*, Apr. 2013, pp. 440–443.
[44] D. He, W. Liu, Y. Ruan, X. Fu, and C. Stefanini, "Preliminary study on piezoresistive and piezoelectric properties of a double-layer soft material for tactile sensing," *Mater. Sci.*, vol. 21, no. 2, pp. 238–243, Jun. 2015, doi: 10.5755/j01.ms.21.2.6454.
[45] S. Khan, W. Dang, L. Lorenzelli, and R. Dahiya, "Flexible pressure sensors based on screen-printed P(VDF-TrFE) and P(VDF-TrFE)/MWCNTs," *IEEE Trans. Semicond. Manuf.*, vol. 28, no. 4, pp. 486–493, Nov. 2015, doi: 10.1109/tsm.2015.2468053.
[46] D. Fraser and J. Potter, "The optimum linear smoother as a combination of two optimum linear filters," *IEEE Trans. Autom. Control*, vol. AC-14, no. 4, pp. 387–390, Aug. 1969, doi: 10.1109/tac.1969.1099196.
[47] D. Hall and S. McMullen, *Mathematical Techniques in Multisensor Data Fusion*. Boston, MA, USA: Artech House, 2004.
[48] E. Wilfried, "An introduction to sensor fusion," Dept. Comput. Eng., Vienna Univ. Technol., Vienna, Austria, Res. Rep. 47/2001, 2002.
[49] Q. Jiang, X. Jin, G. Chen, S.-J. Lee, X. Cui, S. Yao, and L. Wu, "Two-scale decomposition-based multifocus image fusion framework combined with image morphology and fuzzy set theory," *Inf. Sci.*, vol. 541, pp. 442–474, Dec. 2020.
[50] K. Zhang, Y. Huang, X. Yuan, H. Ma, and C. Zhao, "Infrared and visible image fusion based on intuitionistic fuzzy sets," *Infr. Phys. Technol.*, vol. 105, Mar. 2020, Art. no. 103124.
[51] Y. Yang, Y. Que, S. Huang, and P. Lin, "Multimodal sensor medical image fusion based on type-2 fuzzy logic in NSCT domain," *IEEE Sensors J.*, vol. 16, no. 10, pp. 3735–3745, May 2016.
[52] P. Balasubramaniam and V. P. Ananthi, "Image fusion using intuitionistic fuzzy sets," *Inf. Fusion*, vol. 20, pp. 21–30, Nov. 2014.
[53] J. R. Raol, *Multi-Sensor Data Fusion With MATLAB*. Boca Raton, FL, USA: CRC Press, 2010.
[54] E. Nirmala, D. V. Vaidehi, and S. I. Gandhi, "Data fusion using fuzzy logic for multi target tracking," in *Proc. Int. Radar Symp. India*, 2005, pp. 75–80.
[55] S. K. Kashyap and J. R. Raol, "Fuzzy logic applications in filtering and fusion for target tracking," *Defence Sci. J.*, vol. 58, no. 1, pp. 120–135, 2008, doi: 10.14429/dsj.58.1630.
[56] T. J. Ross, *Fuzzy Logic With Engineering Applications*, 4th ed. Hoboken, NJ, USA: Wiley, 2017.
[57] C. C. Lee, "Fuzzy logic in control systems: Fuzzy logic controller. I," *IEEE Trans. Syst., Man, Cybern.*, vol. 20, no. 2, pp. 404–418, Mar./Apr. 1990, doi: 10.1109/21.52551.
[58] M. Sugeno, "An introductory survey of fuzzy control," *Inf. Sci.*, vol. 36, nos. 1–2, pp. 59–83, 1985. Accessed: Oct. 18, 2020, doi: 10.1016/0020-0255(85)90026-x.
[59] Mathworks. (2020). *Sugeno Fuzzy Inference System—MATLAB*. Accessed: Oct. 18, 2020. [Online]. Available: https://www.mathworks.com/help/fuzzy/sugfis.html
[60] *MATLAB Version 9.7.0.1296695 (R2019b) Update 4*, MathWorks, Natick, MA, USA, 2010.
[61] Mathworks. (2020). *Tuning Fuzzy Inference Systems–MATLAB & Simulink*. Accessed: Oct. 18, 2020. [Online]. Available: https://www.mathworks.com/help/fuzzy/tune-fuzzy-inference-systems.html
[62] Mathworks. (2020). *Fuzzy Clustering–MATLAB & Simulink*. Accessed: Oct. 18, 2020. [Online]. Available: https://www.mathworks.com/help/fuzzy/fuzzy-clustering.html
[63] J. C. Bezdek, *Pattern Recognition With Fuzzy Objective Function Algorithms*. New York, NY, USA: Plenum, 1981.
[64] Mathworks. (2020). *Fuzzy C-Means Clustering—MATLAB FCM*. Accessed: Oct. 18, 2020. [Online]. Available: https://www.mathworks.com/help/fuzzy/fcm.html
[65] S. L. Chiu, "Fuzzy model identification based on cluster estimation," *J. Intell. Fuzzy Syst.*, vol. 2, no. 3, pp. 267–278, 1994, doi: 10.3233/ifs-1994-2306.
[66] Mathworks. (2020). *Find Cluster Centers Using Subtractive Clustering—MATLAB Subclust*. Accessed: Oct. 18, 2020. [Online]. Available: https://www.mathworks.com/help/fuzzy/subclust.html
[67] J. M. Mendel, H. Hagras, W. Tan, W. W. Melek and H. Ying, *Introduction to Type-2 Fuzzy Logic Control*. Hoboken, NJ, USA: Wiley, 2014.
[68] Mathworks. (2020). *Convert Type-1 Fuzzy Inference System Into Type-2 Fuzzy Inferencesystem—MATLAB Converttotype2*. Accessed: Oct. 18, 2020. [Online]. Available: https://www.mathworks.com/help/fuzzy/mamfistype2.converttotype2.html
[69] N. N. Karnik and J. M. Mendel, "Centroid of a type-2 fuzzy set," *Inf. Sci.*, vol. 132, nos. 1–4, pp. 195–220, 2001, doi: 10.1016/s0020-0255(01)00069-x.
[70] M. Sugeno, *Industrial Applications of Fuzzy Control*. Amsterdam, The Netherlands: North Holland, 1992.
[71] Mathworks. (2020). *Type-2 Fuzzy Inference Systems–MATLAB & Simulink*. Accessed: Oct. 18, 2020. [Online]. Available: https://www.mathworks.com/help/fuzzy/type-2-fuzzy-inference-systems.html?s_tid=srchtitle